

Are Sampling Heuristics Necessary in Object Detectors?

Joya Chen¹, Dong Liu², Tong Xu^{*1}, and Enhong Chen¹

¹Anhui Province Key Laboratory of Big Data Analysis and Application, University of Science and Technology of China

²CAS Key Laboratory of Technology in Geo-Spatial Information Processing and Application System, University of Science and Technology of China

chenjoya@mail.ustc.edu.cn dongeliu@ustc.edu.cn tongxu@ustc.edu.cn cheneh@ustc.edu.cn

Abstract

The prevalent object detectors to date, such as Faster R-CNN and RetinaNet, are always equipped with a hard or soft sampling heuristics (e.g., under-sampling or Focal Loss), which has been considered as a necessary component for mitigating the foreground-background imbalance thus far. In this report, we challenge this paradigm. Our discovery reveals that, by decoupling objectness estimation from classification to transfer the imbalance, the sampling heuristics could be abandoned in object detectors (e.g., Faster R-CNN, RetinaNet, FCOS), with equivalent performance than their vanilla models. As the sampling heuristics usually introduces laborious hyper-parameters tuning, we expect our discovery could simplify the training procedure of object detectors. Code is available at <https://github.com/ChenJoya/objnessdet>.

1. Introduction

With the resurgence of deep learning [7, 9], convolutional object detectors quickly came to dominate the field of object detection. Among them, early successes include two-stage R-CNN and its successors [3, 19]: the proposal stage [22, 19, 27] rapidly narrows down the number of candidate object locations (e.g., $\sim 100k$) to a small number (e.g., $\sim 1k$), followed by the per-region stage for bounding-box refinement and classification. To pursue high computational efficiency, one-stage detectors [14, 16, 17, 12, 24, 18] abandon the usage of proposal stage but directly recognize objects from dense candidates. In practice, both two-stage and one-stage detectors suffer from the imbalance between foregrounds and backgrounds. Most recently, anchor-free detectors [5, 8, 26, 23, 21, 6, 25] that driven by key-point detection (e.g., center point) gain much attention due to their

simplicity, but they encounter the similar dilemma as the overwhelming number of background points over an image.

To alleviate the foreground-background imbalance, the soft/hard sampling heuristics are widely adopted, such as undersampling in Faster R-CNN [19], Focal Loss in RetinaNet [12] and FCOS [21]. Despite being effective, these schemes are usually heuristic and demand laborious hyper-parameters tuning. For instance, OHEM [20] only selects hard examples and requires setting mini-batch size with positive-negative proportion, whereas Focal Loss [12] reshapes the standard cross-entropy loss by two factors to down-weight the well-classified examples. The GHM [10], however, hypothesizes the very hard examples as outliers and introduce a series of assumptions for gradient harmonizing. As illustrated in [10], it is difficult to define the optimal strategy for addressing the imbalance.

It is natural to ask: *whether the heuristic, complicated sampling heuristics in object detection are necessary?* In this work, we revisit the paradigm and discover that, by appropriate training and inference configurations, state-of-the-art object detectors (Faster R-CNN [19] with FPN [11], RetinaNet [21], FCOS [21]) still achieve competitive accuracy without any sampling heuristics. We summarize the configurations as three guidelines:

- **Decoupling objectness from classification:** In most detectors [19, 14, 17, 12, 4, 24, 15, 21], the classification part is responsible for recognizing C object categories ($C = 80$ in COCO [13]) with a background category. Although simple in design, it will introduce the extreme foreground-background imbalance into the classification part. To protect the part from imbalance, we decouple the objectness from classification: the separated objectness part is supposed to distinguishes foregrounds from backgrounds, whereas the classification part is trained only for foreground examples. In this way, the imbalance is transferred to the object-

ness part at training procedure. During inference, the class-specific score $P(Class)$ is computed by the product of objectness $P(Obj)$ and classification score $P(Class|Obj)$, i.e. $P(Class) = P(Class|Obj) \times P(Obj)$.

- **Biased initialization:** At the beginning of training, we observed that the large number of background examples will generate a large, unstable loss value. To prevent it happening, we use the biased initialization [12] for bias item of objectness branch, to ensure the initial objectness estimation being a low value.

- **Threshold adjustment:** Without sampling heuristics, the overwhelming backgrounds may dominant the training, which results in low-confidence outputs. Consequently, lower threshold should be set for preserving more foregrounds during inference.

In Section 2, we will present experimental results to demonstrate that, without any sampling heuristics, various state-of-the-art object detectors could still achieve competitive detection accuracy, including one-stage (RetinaNet [12]), anchor-free (FCOS [21]) and two-stage (Faster R-CNN [19]) detectors.

2. Experiments

In this section, we present performance comparisons for object detectors with and without sampling heuristics. To discuss the necessary of the sampling heuristics, we pursue minimal changes made to baseline models. Therefore, if not specified, the baselines and hyper-parameters follow the configurations in maskrcnn-benchmark [1], a repository that contains the implementations of Faster R-CNN [19], RetinaNet [12] and FCOS¹ [12].

2.1. RetinaNet without Focal Loss

We first introduce how to train RetinaNet without Focal Loss. By default, training hyper-parameters (e.g., learning rate schedule, batch size, image scale) of our experiments are kept consistency with configuration file of RetinaNet with ResNet-50-FPN backbone in maskrcnn-benchmark, e.g., a learning rate of 0.01 with $1 \times$ schedule [2], a batch size of 16, an input scale of 1333×800 .

Architecture. We introduce how to insert an objectness branch into RetinaNet (*RetinaNet-Obj*) to substitute for Focal Loss (*RetinaNet-FL*). As shown in Figure 1, we simply apply a conv layer on the top of class subnet, which outputs objectness logits p_o in parallel with class-specific logits p_c . Correspondingly, the class subnet is no longer training with background examples, and final class-specific score during inference is computed by $p_o \times p_c$ as well. In this way, we successfully decoupled objectness from classification, which protects the multi-classification part from foreground-background imbalance.

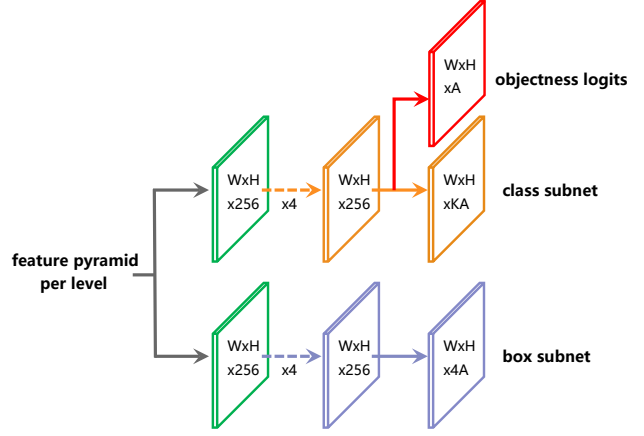


Figure 1. Architecture of RetinaNet with objectness (*RetinaNet-Obj*), which is similar with the original model (*RetinaNet-FL* [12]) but an objectness branch incorporated. The class subnet predicts the class-specific confidence score at each spatial position $W \times H$ for A anchors and K categories, whereas objectness branch estimates objectness score for each anchors.

Initialization. At the beginning of training, we observed that the large number of background examples will generate a large, destabilizing objectness loss. To prevent it happening, we use the biased initialization in [12] to ensure the initial class-specific score and objectness score are $\sim \pi$ ($\pi = 0.01$ by default) and $\sim 1/K$, respectively.

Loss weight. With objectness, the backgrounds no longer incurs classification loss L_{cls} but only for objectness loss L_{obj} , which demands us to tune the weight of them. To keep the consistency with before, we hope the total loss $L_{cls} + L_{reg} + L_{obj}$ close to $L_{cls} + L_{reg}$ in *RetinaNet-FL*. Therefore, we empirically set weights of L_{cls} and L_{obj} to make them similar, and ensure the total loss is similar with the original.

Ablation Studies. Table 1 presents the all experimental results on COCO minival. It illustrates that without Focal Loss, RetinaNet could still achieve competitive accuracy. These results will be discussed in detail as follows.

- **Threshold movement is helpful.** Table 1(a) and (b) show the effect of threshold movement: with appropriate inference threshold, *RetinaNet-Obj* achieved 1.0 AP improvement, while *RetinaNet-FL* also obtained 0.1 higher AP.

- **Objectness and Focal Loss have similar effect.** See Table 1(c), without Focal Loss or objectness, the RetinaNet (*RetinaNet-None*) only achieved 31.1 AP, which is obviously lower than *RetinaNet-FL* (36.4 AP) and *RetinaNet-Obj* (36.5 AP). By replacing Focal Loss with objectness, the degradation in performance did not appear but 0.1 AP improvement was achieved, which illustrates that Focal Loss is unnecessary for addressing the imbalance. Moreover, by applying Focal Loss for objectness, it further improved 0.4 AP (36.5 AP vs. 36.9 AP) in the performance. But this gain is minor, which may be attributed to hard example mining.

¹<https://github.com/tianzhi0549/FCOS>

(a) Varying inference threshold θ (w. optimal NMS η) for *RetinaNet-FL*

Threshold	AP	AP ₅₀	AP ₇₅	AP _S	AP _M	AP _L
$\theta = 0.100, \eta = 0.45$	36.3	55.1	38.9	19.6	40.0	48.9
$\theta = 0.050, \eta = 0.50$	36.4	55.0	39.0	19.9	40.3	48.9
$\theta = 0.010, \eta = 0.50$	36.4	55.0	39.0	19.9	40.3	48.9
$\theta = 0.005, \eta = 0.50$	36.4	55.0	39.0	19.9	40.3	48.9
$\theta = 0.001, \eta = 0.50$	36.4	55.0	39.0	19.9	40.3	48.9

(b) Varying inference threshold θ (w. optimal NMS η) for *RetinaNet-Obj*

Threshold	AP	AP ₅₀	AP ₇₅	AP _S	AP _M	AP _L
$\theta = 0.100, \eta = 0.45$	35.5	53.7	37.8	18.3	38.9	48.3
$\theta = 0.050, \eta = 0.45$	35.9	54.8	38.2	18.9	39.4	48.6
$\theta = 0.010, \eta = 0.45$	36.4	55.7	38.5	19.5	39.9	48.9
$\theta = 0.005, \eta = 0.50$	36.5	55.7	38.7	19.7	40.2	49.0
$\theta = 0.001, \eta = 0.50$	36.5	55.7	38.7	19.8	40.2	49.0

(c) The solution for addressing the imbalance for RetinaNet

Solution	AP	AP ₅₀	AP ₇₅	AP _S	AP _M	AP _L
<i>RetinaNet-None</i>	31.1	48.8	32.8	17.5	34.2	41.0
<i>RetinaNet-FL</i>	36.4	55.0	39.0	19.9	40.3	48.9
<i>RetinaNet-Obj</i>	36.5	55.7	38.7	19.8	40.2	49.0
<i>RetinaNet-FL&Obj</i>	36.9	55.4	39.3	19.9	40.6	48.4

(d) Bias initialization of objectness prior π for *RetinaNet-Obj*

Prior	AP	AP ₅₀	AP ₇₅	AP _S	AP _M	AP _L
$\pi = 0.500$	n/a	n/a	n/a	n/a	n/a	n/a
$\pi = 0.050$	36.5	55.7	38.7	19.8	40.2	49.0
$\pi = 0.010$	36.5	55.7	38.7	19.8	40.2	49.0
$\pi = 0.001$	36.5	55.7	38.7	19.8	40.2	49.0

Table 1. Average Precision (AP) results of *RetinaNet-FL* and *RetinaNet-Obj* on COCO *minival*. If not specified, $\pi = 0.01$, $\lambda = 0.5$, $\theta = 0.001$, $\eta = 0.45$. *RetinaNet-Obj* achieves 36.5 AP at most, which is 0.1 AP higher than the best result (36.4 AP) of *RetinaNet-FL*.

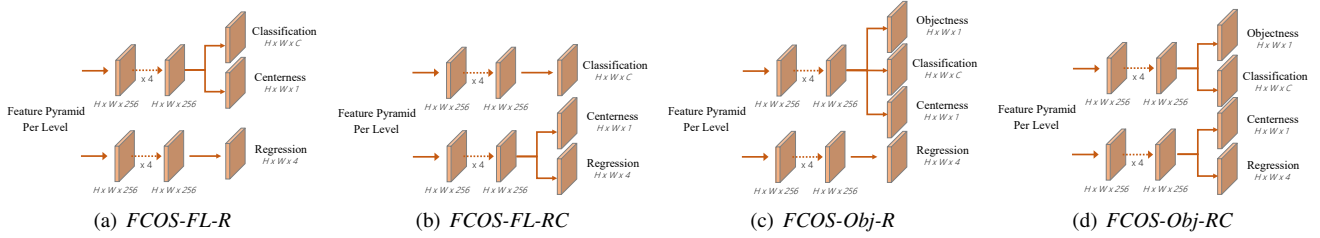


Figure 2. Architectures of FCOS with or without objectness (*FCOS-Obj*, *FCOS-FL*), where the *FCOS-Obj* are similar with the *FCOS-FL* but an objectness incorporated, yielding C object categories, 1 centerness score, 1 objectness score and 4 location coordinates at each pixel. We rearrange centerness branch for preventing head network from being too heavy.

• **Biased initialization is robust to exact value.** As presented in Table 1(d), our first attempt to train *RetinaNet-Obj* used no biased initialization, which failed quickly, with the network diverging during training. However, simply initializing the prior probability of objectness to $\pi = .05$ or lower value, the training became effective. It suggests that the biased initialization is crucial for training *RetinaNet-Obj*, but the results are insensitive to the exact prior probability.

Conclusions. In the above, we have presented that the *RetinaNet-Obj* and *RetinaNet-FL* could achieve comparable COCO AP results. The three guidelines — *decoupling objectness from classification*, *biased initialization*, *threshold movement* not only make it possible to train without sampling heuristics, but also improve the accuracy of RetinaNet. In the next section, we will continue to validate them on other detectors.

2.2. FCOS without Focal Loss

In this section, we focus on how to train an anchor-free detector FCOS [21] without Focal Loss, and achieve similar performance than that with Focal Loss as well. Its training hyper-parameters (e.g., learning rate schedule, batch size, image scale) are kept consistency with configuration file of FCOS with ResNet-50-FPN backbone in *maskrcnn-benchmark*, e.g., a learning rate of 0.01 with $1 \times$ schedule [2], a batch size of 16, an input scale of 1333×800 .

Architecture. As FCOS has a centerness branch in parallel with classification, inserting objectness branch here is more complicated than that in RetinaNet. As shown in Figure 2, we arrange the centerness and objectness branches to different position, to prevent the subnet from being too heavy. Correspondingly, in ablation studies, we will compare *FCOS-FL-CC* with *FCOS-Obj-CC*, as well as *FCOS-FL-C* with *FCOS-Obj-CC*.

Training and Inference Configurations. Following Section 2.1, we use the three guidelines here to train FCOS without Focal Loss. First, we decouple the objectness from classification (see Figure 2), and make the classification part trained only for foreground pixels as well. Then, we initialize objectness branch by a low value, to avoid network diverging. As it is robust to exact prior probability, we simply set $\pi = 0.01$ here. Finally, during inference, threshold movement is adopted for achieving the best performance.

Results. As shown in Table 2, we conducted thoughtful experiments for illustrating that FCOS without Focal Loss could also achieve similar accuracy. Table 2(a) shows that for *FCOS-CC* architecture, there is only 0.3 AP gap between *RetinaNet-Obj* and *RetinaNet-FL*. In Table 2(b), this gap narrows down to 0.1 AP, as the *FCOS-C* architecture protects the subnet containing objectness branch from being too heavy. In conclusion, the experimental results demonstrate that Focal Loss is not necessary for FCOS.

(a) Architecture comparison for *FCOS-FL*

Branch	AP	AP ₅₀	AP ₇₅	AP _S	AP _M	AP _L
<i>FCOS-None-R</i>	33.5	52.6	35.2	20.8	38.5	42.6
<i>FCOS-FL-R</i>	37.0	55.8	39.5	21.4	40.9	47.8
<i>FCOS-Obj-R</i>	36.7	55.6	39.2	20.8	41.2	47.2

(b) Architecture comparison for *FCOS-Obj*

Branch	AP	AP ₅₀	AP ₇₅	AP _S	AP _M	AP _L
<i>FCOS-None-RC</i>	33.8	52.4	35.6	20.8	38.7	44.4
<i>FCOS-FL-RC</i>	37.2	55.6	40.1	21.3	41.0	49.5
<i>FCOS-Obj-RC</i>	37.1	55.9	39.9	21.2	40.9	48.8

Table 2. Average Precision (AP) results of *FCOS-FL* and *FCOS-Obj* with different architectures on COCO *minival*. The effect of Focal Loss and objectness is very similar (≤ 0.3 AP). Compared with Table (a) and (b), we can see that by the centerness being parallel with regression, the *FCOS-Obj* could achieve higher performance that being comparable with *FCOS-FL*.

Stage	undersampling			
RPN	✓	✗	✓	✗
RoI-subnet	✓	✓	✗	✗
AP	36.8	37.2 (+0.4)	36.7 (-0.1)	37.2 (+0.4)
AP ₅₀	58.4	58.7 (+0.3)	58.3 (-0.1)	58.7 (+0.3)
AP ₇₅	40.0	40.0 (+0.0)	39.7 (-0.3)	40.2 (+0.2)
AP _S	20.7	21.3 (+0.6)	21.7 (+1.0)	21.6 (+0.9)
AP _M	39.7	40.3 (+0.6)	39.7 (+0.0)	40.6 (+0.9)
AP _L	47.9	48.6 (+0.7)	48.0 (+0.1)	48.3 (+0.4)

Table 3. Ablation studies for our overlap sampler.

2.3. Faster R-CNN without Sampling Heuristics

In the above, we have introduced for one-stage (RetinaNet) and anchor-free (FCOS) detectors, the reweighting scheme Focal Loss for addressing the imbalance may not be the necessary. Now, we discuss whether the sampling heuristics (undersampling in maskrcnn-benchmark) for region-based detectors is substitutable. Following standard practices, training hyper-parameters (e.g., learning rate schedule, batch size, image scale) of our experiments are kept consistency with configuration file of Faster R-CNN with ResNet-50-FPN backbone in maskrcnn-benchmark, e.g., a learning rate of 0.02 with $1 \times$ schedule [2], a batch size of 16, an input scale of 1333×800 .

Initialization. The RPN has two tasks: objectness estimation and bounding-box regression. After abandoning the usage of undersampling, the overwhelming number of backgrounds will generate a large, destabilizing objectness loss. To prevent it happening, we use the biased initialization in [12] to ensure the initial objectness score is ~ 0.01 , although results are robust to the exact value, which has been demonstrated in Table 1.

Training and Inference Configurations. We empirically tuned the weight of objectness loss to keep the consistency with the original loss, as did in Section 2.1 and Section 2.2.

Results. As presented in Table 3, the original Faster R-CNN, which adopts undersampling in RPN and RoI-Net, achieved 36.8 AP on COCO *minival*. Then, we gradually abandon the usage of undersampling and observe the changes in performance. It shows that without undersampling in RPN, Faster R-CNN achieves surprisingly 0.4 AP higher than the vanilla model. As the RPN suffers from extreme foreground-background imbalance, this result sug-

gests that the undersampling is unnecessary for region proposal stage, which has not been explored before.

Nevertheless, with RPN to remove backgrounds, the remaining candidates in RoI-Net still contain a large number of backgrounds, which results in the undersampling to be reused in per-region stage in the vanilla Faster R-CNN. Therefore, we investigate whether the sampling paradigm could be abandoned in RoI-Net. As shown in the third column of Table 3, by replacing sampling heuristic with objectness, the detector achieves a very similar result compared with the original (36.7 AP vs. 36.8 AP). Moreover, while the undersampling is not used both in RPN and RoI-Net, the Faster R-CNN achieves 37.2 AP, which is 0.4 AP higher than the vanilla Faster R-CNN. Although undersampling have been viewed as an essential component for addressing the imbalance, our report challenges this paradigm: by three simple training and inference guidelines, the undersampling could be entirely abandoned for region proposal and per-region stages, but a similar or even higher accuracy could be achieved.

3. Conclusion

In this technical report, we investigated in object detectors, whether the sampling heuristics for addressing the imbalance are necessary. Our experiments surprisingly presented, with three rules — *decoupling objectness from classification*, *biased initialization*, *threshold movement* — guided training and inference, various object detectors (two-stage, one-stage or anchor-free) still achieved competitive accuracy without any sampling heuristics. We sincerely hope the experimental evidence here will facilitate future research.

References

- [1] Massa Francisco and Girshick Ross. maskrcnn-benchmark: Fast, modular reference implementation of Instance Segmentation and Object Detection algorithms in PyTorch. <https://github.com/facebookresearch/maskrcnn-benchmark>, 2018. Accessed: [July 21, 2019].
- [2] Ross Girshick, Ilija Radosavovic, Georgia Gkioxari, Piotr Dollár, and Kaiming He. Detectron. <https://github.com/facebookresearch/detectron>, 2018.

- [3] Ross B. Girshick. Fast R-CNN. In *ICCV*, pages 1440–1448, 2015.
- [4] Kaiming He, Georgia Gkioxari, Piotr Dollár, and Ross B. Girshick. Mask R-CNN. In *ICCV*, pages 2980–2988, 2017.
- [5] Lichao Huang, Yi Yang, Yafeng Deng, and Yinan Yu. Densebox: Unifying landmark localization with end to end object detection. *CoRR*, abs/1509.04874, 2015.
- [6] Tao Kong, Fuchun Sun, Huaping Liu, Yuning Jiang, and Jianbo Shi. Foveabox: Beyond anchor-based object detector. *CoRR*, abs/1904.03797, 2019.
- [7] Alex Krizhevsky, Ilya Sutskever, and Geoffrey E. Hinton. Imagenet classification with deep convolutional neural networks. *Commun. ACM*, 60(6):84–90, 2017.
- [8] Hei Law and Jia Deng. Cornernet: Detecting objects as paired keypoints. In *ECCV*, pages 765–781, 2018.
- [9] Yann LeCun, Yoshua Bengio, and Geoffrey E. Hinton. Deep learning. *Nature*, 521(7553):436–444, 2015.
- [10] Buyu Li, Yu Liu, and Xiaogang Wang. Gradient harmonized single-stage detector. In *AAAI*, pages 8577–8584, 2019.
- [11] Tsung-Yi Lin, Piotr Dollár, Ross B. Girshick, Kaiming He, Bharath Hariharan, and Serge J. Belongie. Feature pyramid networks for object detection. In *CVPR*, pages 936–944, 2017.
- [12] Tsung-Yi Lin, Priya Goyal, Ross B. Girshick, Kaiming He, and Piotr Dollár. Focal loss for dense object detection. In *ICCV*, pages 2999–3007, 2017.
- [13] Tsung-Yi Lin, Michael Maire, Serge J. Belongie, James Hays, Pietro Perona, Deva Ramanan, Piotr Dollár, and C. Lawrence Zitnick. Microsoft COCO: common objects in context. In *ECCV*, pages 740–755, 2014.
- [14] Wei Liu, Dragomir Anguelov, Dumitru Erhan, Christian Szegedy, Scott E. Reed, Cheng-Yang Fu, and Alexander C. Berg. SSD: single shot multibox detector. In *ECCV*, pages 21–37, 2016.
- [15] Jiangmiao Pang, Kai Chen, Jianping Shi, Huajun Feng, Wanli Ouyang, and Dahua Lin. Libra R-CNN: towards balanced learning for object detection. *CoRR*, abs/1904.02701, 2019.
- [16] Joseph Redmon, Santosh Kumar Divvala, Ross B. Girshick, and Ali Farhadi. You only look once: Unified, real-time object detection. In *CVPR*, pages 779–788, 2016.
- [17] Joseph Redmon and Ali Farhadi. YOLO9000: better, faster, stronger. In *CVPR*, pages 6517–6525, 2017.
- [18] Joseph Redmon and Ali Farhadi. Yolov3: An incremental improvement. *CoRR*, abs/1804.02767, 2018.
- [19] Shaoqing Ren, Kaiming He, Ross B. Girshick, and Jian Sun. Faster R-CNN: towards real-time object detection with region proposal networks. *IEEE Trans. Pattern Anal. Mach. Intell.*, 39(6):1137–1149, 2017.
- [20] Abhinav Shrivastava, Abhinav Gupta, and Ross B. Girshick. Training region-based object detectors with online hard example mining. In *CVPR*, pages 761–769, 2016.
- [21] Zhi Tian, Chunhua Shen, Hao Chen, and Tong He. FCOS: fully convolutional one-stage object detection. *CoRR*, abs/1904.01355, 2019.
- [22] Jasper R. R. Uijlings, Koen E. A. van de Sande, Theo Gevers, and Arnold W. M. Smeulders. Selective search for object recognition. *International Journal of Computer Vision*, 104(2):154–171, 2013.
- [23] Jiaqi Wang, Kai Chen, Shuo Yang, Chen Change Loy, and Dahua Lin. Region proposal by guided anchoring. *CoRR*, abs/1901.03278, 2019.
- [24] Shifeng Zhang, Longyin Wen, Xiao Bian, Zhen Lei, and Stan Z. Li. Single-shot refinement neural network for object detection. In *CVPR*, pages 4203–4212, 2018.
- [25] Xingyi Zhou, Dequan Wang, and Philipp Krähenbühl. Objects as points. *CoRR*, abs/1904.07850, 2019.
- [26] Xingyi Zhou, Jiacheng Zhuo, and Philipp Krähenbühl. Bottom-up object detection by grouping extreme and center points. *CoRR*, abs/1901.08043, 2019.
- [27] C. Lawrence Zitnick and Piotr Dollár. Edge boxes: Locating object proposals from edges. In *ECCV*, pages 391–405, 2014.